https://ntrs.nasa.gov/search.jsp?R=19900017469 2020-03-19T21:18:12+00:00Z

ORIGINAL PAGE IS
OF POOR QUALITY

NONPOTENTIAL MAGNETIC FIELDS AT SITES OF GAMMA-RAY FLARES

M. J. Hagyard
Space Science Laboratory, Marshall Space Flight Center
P. Venkatakrishnan
Indian Institute of Astrophysics
J. B. Smith, Jr.
University of Alabama in Huntsville

1989 FEB 16 A 8:37

Abstract

In this paper the relation between the degree of nonpotentiality of photospheric magnetic fields and the occurrence of gamma-ray flares is examined. We use the parameter $\Delta\Phi$ (termed magnetic "shear") and the strength of the magnetic field intensity as measures of the degree of nonpotentiality, where $\Delta\Phi$ is defined as the angular difference between the observed direction of the transverse component of the photospheric field and the direction of the potential field prescribed by the distribution of measured photospheric flux. An analysis of the great flare of April 24-25, 1984 is presented as an example of this technique to quantify the nonpotential characteristics of the pre-flare magnetic field. For this flare, which produced a large gamma-ray event, we found that strong shear and high field strengths prevailed over an extended length of the magnetic neutral line where the flare occurred. Moreover, the flare began near the area of strongest measured shear (89 - 90 degrees). Four other flaring regions were analyzed; one of these produced a moderate gamma-ray event while the other three did not produce detectable gamma rays. For all four regions the flares were located in the area where the field was most nonpotential, regardless of the class of flare. The fields of the gamma-ray flares were compared with those associated with the flares without gamma rays, and we found little distinction in the degree of magnetic shear. The major difference is seen in the extent of the sheared field: for gamma-ray events, the field is sheared over a longer length of the neutral line.

I. INTRODUCTION

The source of energy of all flares is assumed to be the free energy stored in nonpotential magnetic fields concentrated along and near the magnetic "neutral line" separating fields of opposite polarity in solar active regions. With the advent of measurements of the transverse component of the Sun's photospheric magnetic field with instruments such as the Marshall Space Flight Center's vector magnetograph (Hagyard *et al.* 1982, 1985), quantitative evaluations of the nonpotential nature of these fields can now be made. The line-of-sight component of the photospheric field can determine the structure of the potential field appropriate to that particular distribution of magnetic flux. This potential field can then be compared with the observed transverse field to determine where the field has been stressed into nonpotential configurations. Using this quantitative technique, we

(NASA-TM-100429) NONPOTENTIAL MAGNETIC FIELDS AT SITES OF GAMMA RAY FLARES (NASA) 18 p
CSCL 03B
N90-26785
Unclas
G3/92 0292737

have analyzed MSFC observations of a number of flares observed during the last solar maximum period. Collectively, these analyses have shown that the magnetic field at the sites of ribbon flares is strongly nonpotential, and there is a statistical correlation between increased magnetic stress and increased flare activity (Hagyard *et al.* 1984, 1986).

In this paper we use a similar analysis to investigate the nonpotential characteristics of gamma-ray flares and determine whether there are special signatures of these stressed fields for this special class of flares. We present the results of an analysis of the active region of April 1984, AR4474, which produced one of the most intense flares of the last solar cycle on April 24. This study showed that the big flare initiated at the location on the magnetic neutral line where the field deviated the most from a potential field. We then compare the nonpotential signatures of AR4474 with those of four other regions, one which produced a gamma-ray event and three which did not. Our tentative conclusion from this small data sample is that gamma-ray flares are associated with strongly nonpotential fields which extend over relatively larger lengths of the magnetic neutral line than the fields associated with flares producing no gamma-ray events.

II. ANALYSIS OF THE MAGNETIC FIELD OF ACTIVE REGION AR4474

The active region, designated AR4474 by NOAA, rotated onto the solar disk on April 22, 1984. The great flare erupted on the 24th at 23:57 UT and attained its maximum phase at 23:59 UT (Kurokawa *et al.* 1987). White-light brightenings appeared four minutes after the onset of the flare (Hiei, Zirin and Wang 1986) which was classified as a 3B/X13 event and was one of the most intense flares observed by the SMM Gamma Ray Spectrometer.

Observations of the photospheric magnetic field of this active region were carried out with the MSFC vector magnetograph starting on the 24th at 22:11 UT; the last set of data was obtained near sunset, at 22:36 UT, 80 minutes prior to the onset of the great flare. The overall configuration of the line-of-sight component $B_{\parallel}$ of the magnetic field of AR4474 at 22:11 UT is shown in Figure 1 along with white-light and Hα images taken early and late on the 24th and again early on the 25th at the Hida Observatory (Kurokawa *et al.* 1987). Figure 2 shows the development of the flare along the western part of the magnetic neutral line outlined in Figure 1 on the map of $B_{\parallel}$. In Figure 3 the transverse component $B_{\perp}$ of the magnetic field in the area of the flare is shown in the middle panel (b) superposed on the $B_{\parallel}$ field. In the lower panel (c) the potential field determined by $B_{\parallel}$ is displayed in a similar format. Comparison of the observed (b) and potential (c) fields along that portion of the neutral line bracketed by the flare ribbons seen in the top panel (a) demonstrates that the observed field is highly nonpotential there.

This alignment of the transverse field more nearly parallel to the neutral line rather than perpendicular as in the case of the potential field leads to the terminology of magnetic "shear". Studies of the proper motions of the spots in this region by Kurokawa *et al.* (1987) and Gesztelyi and Kalman (1986) clearly indicate that the sheared configuration of the transverse field connecting the opposite polarities across the western section of the magnetic neutral line was probably formed in response to the westward motion of the negative-polarity sunspot located in the lower right part of Figure 3.

With the data shown in Figure 3 we can characterize the magnetic shear in a quantitative way by calculating the parameter $\Delta\Phi$, defined as the difference between the observed

ORIGINAL PAGE IS
OF POOR QUALITY

direction of the transverse field and the direction of the transverse potential field. If the field is nearly potential, then $\Delta\Phi \approx 0°$; for a highly sheared field, $\Delta\Phi \approx 90°$. In the analysis scheme, we identify the string of points forming the neutral line and calculate $\Delta\Phi$ at those points where the transverse field strength is above 200 G. To display the results we use the following criteria to select ranges of shear: $B_T \geq \frac{1}{2}B_T^{max}$ and $70° \leq \Delta\Phi < 80°$, $B_T \geq \frac{1}{2}B_T^{max}$ and $\Delta\Phi \geq 80°$, where B_T^{max} is the maximum field intensity along the relevant portion of the neutral line.

Figure 4 is a magnetic shear map of the data obtained at 22:36 UT. The dots indicate neutral-line points where $B_T > 200$ G, the open circles indicate points consistent with the first criterion, and the filled squares indicate those consistent with the second one.

To allay concerns that projection effects might render these analyses invalid since the region was at a longitude offset of $-45°$, we carried out the same calculations after transforming the magnetic field components from the image-plane frame of reference to heliographic coordinates (Venkatakrishnan, Hagyard and Hathaway 1988a). The results obtained (Venkatakrishnan, Hagyard and Hathaway 1988b) showed only a minor change: one less circle and one less square in the heliographic coordinate system.

An earlier magnetogram, taken at 22:11 UT was analyzed and compared with the later one to look for indications of an evolution of the shear; the resulting shear map is shown in Figure 5. In Table 1 the numerical values for B_T and $\Delta\Phi$ are given for the 15 points that correspond to the 15 circles and squares seen in Figures 4 and 5 along the western neutral line, starting with the northern 3 consecutive circles.

TABLE 1
Magnetic Intensity and Shear at Points
along the Western Neutral Line

	22:11 UT		22:36 UT	
Point	B_T(G)	$\Delta\Phi$	B_T(G)	$\Delta\Phi$
1	1225	73°	1315	70°
2	1325	73°	1380	72°
3	1320	77°	1355	79°
4	1235	83°	1255	89°
5	1110	89°	1140	89°
6	1095	89°	1155	80°
7	1180	90°	1230	82°
8	1360	84°	1370	84°
9	1360	81°	1415	79°
10	1590	82°	1550	86°
11	1715	82°	1640	90°
12	1725	87°	1555	86°
13	1420	83°	1335	79°
14	1360	77°	1240	86°
15	1055	75°	980	84°

ORIGINAL PAGE IS
OF POOR QUALITY

Comparing Figures 4 and 5 and looking at the numerical data given in the table, there does not seem to be any *overall* trend of a general increase or decrease in field strength or shear. All but two of the changes in field strength lie below the calculated noise level of 135 G for B_T and are therefore not significant. In the case of the shear parameter $\Delta\Phi$, the uncertainty in Φ was calculated to be $\approx 1-2°$ for field strengths on the order of 1000 G. Thus we might take changes of 4° or more as significant if they occur at two or more consecutive pixels. Using this criterion, there is an indication of a decrease in shear at points 6 and 7, an increase at points 10 and 11, and an increase at points 14 and 15. To feel comfortable with designating these changes as truly significant, we would find it more reassuring if more than two consecutive points were involved. A conservative conclusion is that there is no extended region of increasing or decreasing shear.

Kurokawa *et al.* indicate that the first Hα brightenings of the flare were near the filament in the region of the neutral line to the north of the large negative spot and east of the positive spot seen in Figures 4 and 5. This seems to place the location of flare onset near points 4 - 7 of Table 1. The flare then spread along the neutral line between the two sunspots. Thus the flare began near points having the strongest measured shear (89° - 90°) prior to the flare and enveloped the whole area of strong shear and high field strength shown in Figures 4 and 5.

Magnetograph observations were obtained on April 25 at 16:25 UT, but instrumental problems that occurred have made it difficult to properly analyze the data for the post-flare configuration of the photospheric field. Thus we cannot say at this time whether there was a change in the degree of nonpotentiality as a result of the large flare.

This same region produced a number of flares over the next five days, including a dozen M-class x-ray events and four flares classed as 2B. One of these latter occurred on April 28 at 20:17 UT. This particular flare, a 2B/C6 event, was located in the *eastern* portion of AR4474, in the other area of significant shear seen in Figures 4 and 5. We analyzed a magnetogram taken at 19:53 UT, 24 minutes before the flare started; the shear map for this magnetogram is shown in Figure 6. There are two noteworthy points to be made about the areas of shear seen in this map. First, the large area of shear in the western spots - the region of the gamma-ray event on the 24^{th} - has persisted and indicates that this area is more nonpotential than the eastern region. However, in the time interval of 20:00 UT $\pm$ 4 h, only subflares were observed there. This observation supports the idea that large shear alone is not a sufficient condition for flaring. The second point is that the shear in the eastern area on the 28^{th} has increased from the values calculated on the 24^{th}; this increase can be seen by comparing Figures 4 and 5 with Figure 6. Remembering that large shearing motions occurred in the *western* area in the period 23 to 24 April before the gamma-ray flare and noting that an increase in shear took place between 24 and 28 April in the eastern area before the flare there, we conclude that increases in the length of the critically sheared region over a timescale of a few days could herald the onset of major flares.

The flare on April 28 was not a gamma-ray event although it was a large flare by most standards. In comparing the nonpotential characteristics of the two areas of AR4474, the significant difference between the area of the gamma-ray flare and the other highly sheared region is the length of the neutral line involved. In the next section we will investigate

ORIGINAL PAGE IS
OF POOR QUALITY

whether this criterion holds for other active regions that we have analyzed.

III. ANALYSIS OF SHEAR FOR OTHER CLASSES OF FLARES

Similar analyses have been carried out for three other active regions of the last solar cycle; each of these regions produced a series of major flares. The first region, designated AR4711, produced a major flare - 3B/X3 - and a gamma-ray event on February 4, 1986, at 07:41 UT. The pre-flare magnetic field was measured with the MSFC magnetograph at 16:42 UT on February 3^{rd}; the image-plane map of the shear parameter $\Delta\Phi$ is shown in Figure 6. The flare occurred on that part of the neutral line where the 9 solid squares and 1 open circle are located. Moreover the initial flare brightenings were located in the area where there was maximum angular shear.

In Figure 7 the shear map for AR2776 at 14:23 UT on November 5, 1980 is shown. This data set preceded a 1B/M2 flare at 16:03 UT, the first major flare produced in this active region. The location of this flare again coincides with the area where the field was the most nonpotential, i.e., where there was a coincidence of large shear and strong fields as indicated by the 7 solid squares and 1 open circle. Here, too, the initial flare kernels were seen to bracket the neutral line where $\Delta\Phi$ was largest.

The last region, AR2372, which was on the solar disk in April 1980, produced a number of M-class flares and one X-class event in the period April 5-8. The magnetic data that were analyzed for shear were obtained in the middle of this period at 21:10 UT on the 6^{th}. The next major flare following the magnetic observations was a 1B/M4 event at 00:48 UT on the 7^{th}. The shear map for the observations at 21:10 UT is displayed in Figure 8. There are 2 areas of strong shear as defined by our criteria, and both were locations of flare ribbons. However, the flare onset was observed at the area of 3 solid squares and 5 open circles, and this is where the field intensity was highest and the shear strongest.

The results of these analyses are summarized in Table 2 where we have indicated for each flare the maximum observed transverse field strength on the relevant section of the magnetic neutral line (Max B_T), the maximum shear along that neutral line (Max $\Delta\Phi$), the maximum number of *consecutive* points designated by open circles and filled squares (No. points), the flare class, and whether there was a gamma-ray event detected.

TABLE 2
Comparison of Nonpotentiality Parameters
for Different Flares

Date of Flare	Max B_T	Max $\Delta\Phi$	No. Points	Flare Class	γ Event
4/24/84	1700 G	90°	15	3B/X13	yes!
4/28/84	1920 G	90°	8	2B/C6	no
2/04/86	1100 G	90°	10	3B/X3	yes
11/5/80	1000 G	88°	8	1B/M2	no
4/07/80	1000 G	85°	8	1B/M4	no

IV. SUMMARY AND CONCLUSIONS

ORIGINAL PAGE IS
OF POOR QUALITY

The results of this study indicate that for all four active regions studied, the five flares were located in an area where the magnetic field deviated the most from a potential field, regardless of the class of flare. In addition, flare onset appears to occur preferentially at the point of greatest shear $\Delta\Phi$. However, there doesn't seem to be any distinctive difference in the degree of shear between flares that produce gamma-ray events and those that do not. A similar inference seems to pertain to the strength of the field. There does seem to be an indication that the gamma-event flares occur where strongly nonpotential fields extend over a relatively large area. This conclusion is based on the result that the number of consecutive points of high shear and strong fields is larger for the two gamma-ray flares of 24 April 1984 and February 1986. Obviously, many more cases need to be analyzed before we can make a definitive statement as to the existence of any special signatures of gamma-ray flares that are seen in the magnetic field.

This work was done while one of us (P. V.) held a National Research Council - NASA Research Associateship. The observational programs that produced the magnetic data reported in this paper were carried out as part of the Solar Maximum Mission Guest Investigator Program. Support for this research was provided by NASA through its Solar Physics Branch of the Space Physics Division and by the Air Force Geophysical Laboratory through its Solar Research Branch of the Space Physics Division.

ORIGINAL PAGE IS
OF POOR QUALITY

REFERENCES

Gesztelyi, L., and Kalman, B. 1986, *Adv. Space Res.*, Vol. 6, No. 6.

Hagyard, M. J., Cumings, N. P., West, E. A., and Smith, J. E. 1982, *Solar Phys.*, 80, 33.

Hagyard, M. J., Cumings, N. P., and West, E. A. 1985, in *Proceedings of Kunming Workshop on Solar Physics and Interplanetary Travelling Phenomena*, ed. C. De Jager and Chen Biao (Beijing: Science Press), p. 204.

Hagyard, M. J., Smith, J. B., Jr., Teuber, D., and West, E. A. 1984, *Solar Phys.*, 91, 115.

Hagyard, M. J., *et al.* 1986, in *Energetic Phenomena on the Sun*, ed. M. R. Kundu and B. E. Woodgate (NASA CP-2439), p. 1-16.

Hiei, E., Zirin, H., and Wang, J. 1986, in *The Lower Atmosphere of Solar Flares*, ed. D. F. Neidig (Sunspot, NM: National Solar Observatory), p. 129.

Kurokawa, H., Hanaoka, Y., Shibata, K., and Uchida, Y. 1987, *Solar Phys.*, 108, 251.

Venkatakrishnan, P., Hagyard, M. J., and Hathaway, D. H. 1988a, *Solar Phys.*, 115, 125.

Venkatakrishnan, P., Hagyard, M. J., and Hathaway, D. H. 1988b, *Solar Phys.*, submitted.

ORIGINAL PAGE IS
OF POOR QUALITY

FIGURE CAPTIONS

Figure 1. Morphology of active region AR4474 near the time of the great flare on April 24, 1984. In the upper image, a line-of-sight ($B_{\|}$) magnetogram taken with the Marshall Space Flight Center's vector magnetograph at 22:11 UT is displayed as contours of positive (solid curves) and negative (dashed curves) fields over a 5′ x 5′ field of view. The major magnetic neutral lines are indicated by the heavier solid lines. The "western section" of the neutral line, where the 3B/X13 white-light flare erupted, lies between the opposite polarities at the center of the image. In the lower panels, the active region is seen in white-light and Hα images obtained from the Hida Observatory.

Figure 2. Development of the great flare of 24 April 1984. These images show how the flare ribbons bracket the western portion of the magnetic neutral line shown in Figure 1. These images were obtained at the Big Bear Solar Observatory.

Figure 3. Nonpotential fields in the region of the great flare of 24 April 1984. The flare ribbons shown in panel a (from the Big Bear Image seen in Figure 2) bracket the magnetic neutral line seen in the vector magnetogram of panel b; the magnetogram was obtained at 22:11 UT, 105 minutes prior to the onset of the flare. In this magnetogram the strength and direction of the transverse component (B_T) of the observed field are indicated by the length and orientation of the line segments which are superimposed on the line-of-sight field. In panel c, the transverse component of the potential field is displayed in the same format. From a comparison of panels b and c we recognize that the observed field along the neutral line in the flaring area is highly nonpotential or "sheared."

Figure 4. A map of the magnetic shear along the neutral line of AR4474 on 24 April. Locations of high magnetic shear on the neutral line of the vector magnetogram obtained at 22:36 UT are indicated by the open circles and solid squares. The meaning of these symbols is given in the text. Note the extended length of high magnetic shear in the area of the great flare.

Figure 5. Persistence of high shear at the flare site on 24 April. This map is similar in format to that of Figure 4 but was derived from a vector magnetogram taken 25 minutes earlier.

Figure 6. Magnetic shear along the neutral line of AR 4474 on 28 April. This map was derived from a vector magnetogram obtained 24 minutes before the 2B/C6 flare at 20:17 UT. The field of view is 230″ x 230″ and west is to the right on the figure.

Figure 7. Magnetic shear map for AR4711. This shear map was derived from a vector magnetogram obtained several hours prior to a 3B/X3 flare. The flare was centered along that portion of the neutral line where the shear was concentrated, as indicated by the solid squares. The field of view is 135″ x 135″ and west is to the left of the image.

Figure 8. Magnetic shear map for AR2776. The first major flare from this region, a 1B/M2 event at 16:03 UT on November 5, was located where this map indicates the highest shear existed. The field of view is 140″ x 140″ and west is to the right.

Figure 9. Magnetic shear map for AR2372. Flare ribbons of the 1B/M4 flare which occurred several hours after the magnetic field observations were made were located at both sites of high shear seen in this map. However, the flare onset was located in the area of the more extended length of shear. The field of view is 125″ x 125″ and west is down.

ORIGINAL PAGE IS
OF POOR QUALITY

Fig. 1

AR 4474
APRIL 24, 1984
SITE OF 3B/X15 FLARE

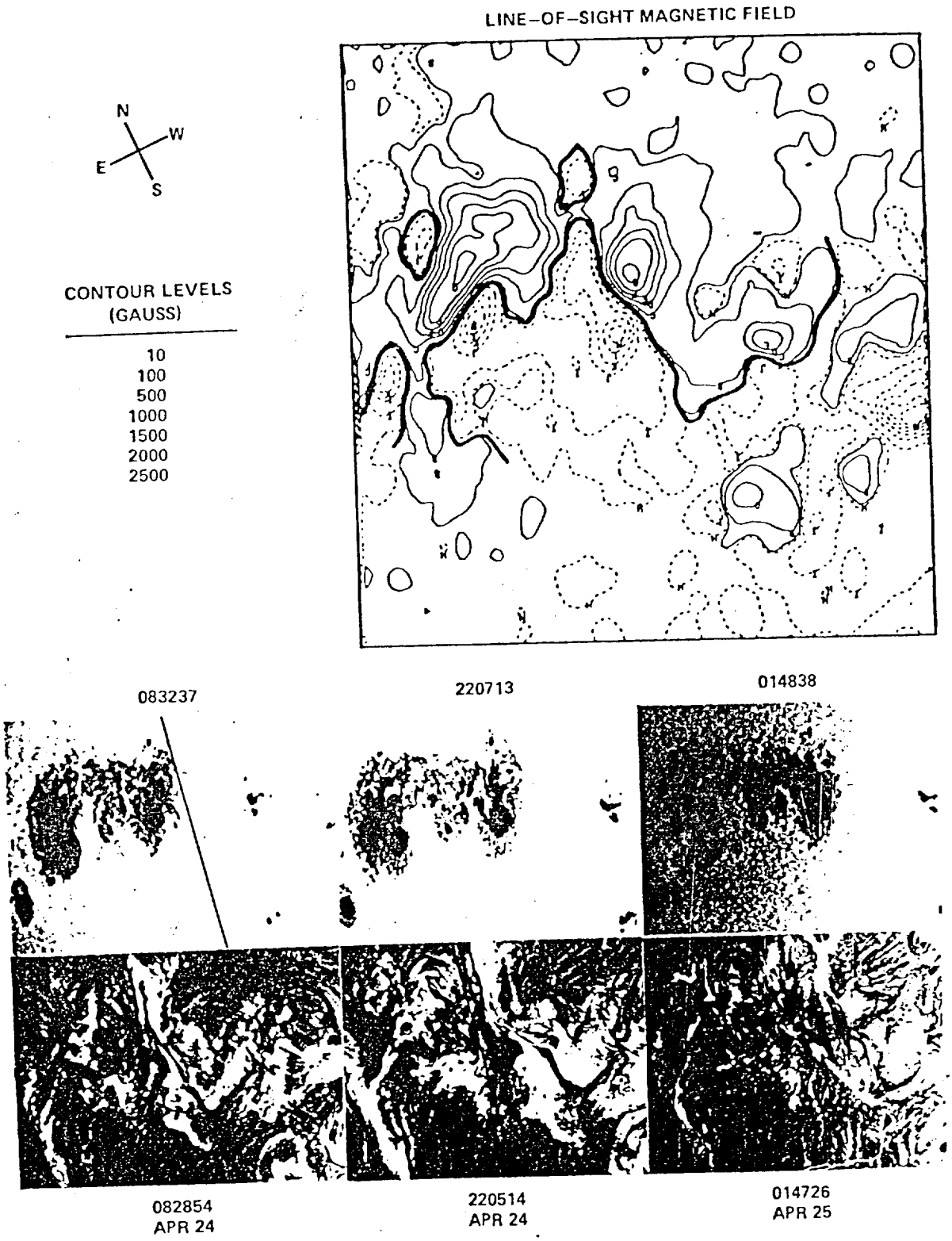

ORIGINAL PAGE IS
OF POOR QUALITY

Fig. 2

3B/X15 FLARE IN AR 4474
APRIL 24-25, 1984
BIG BEAR SOLAR OBSERVATORY

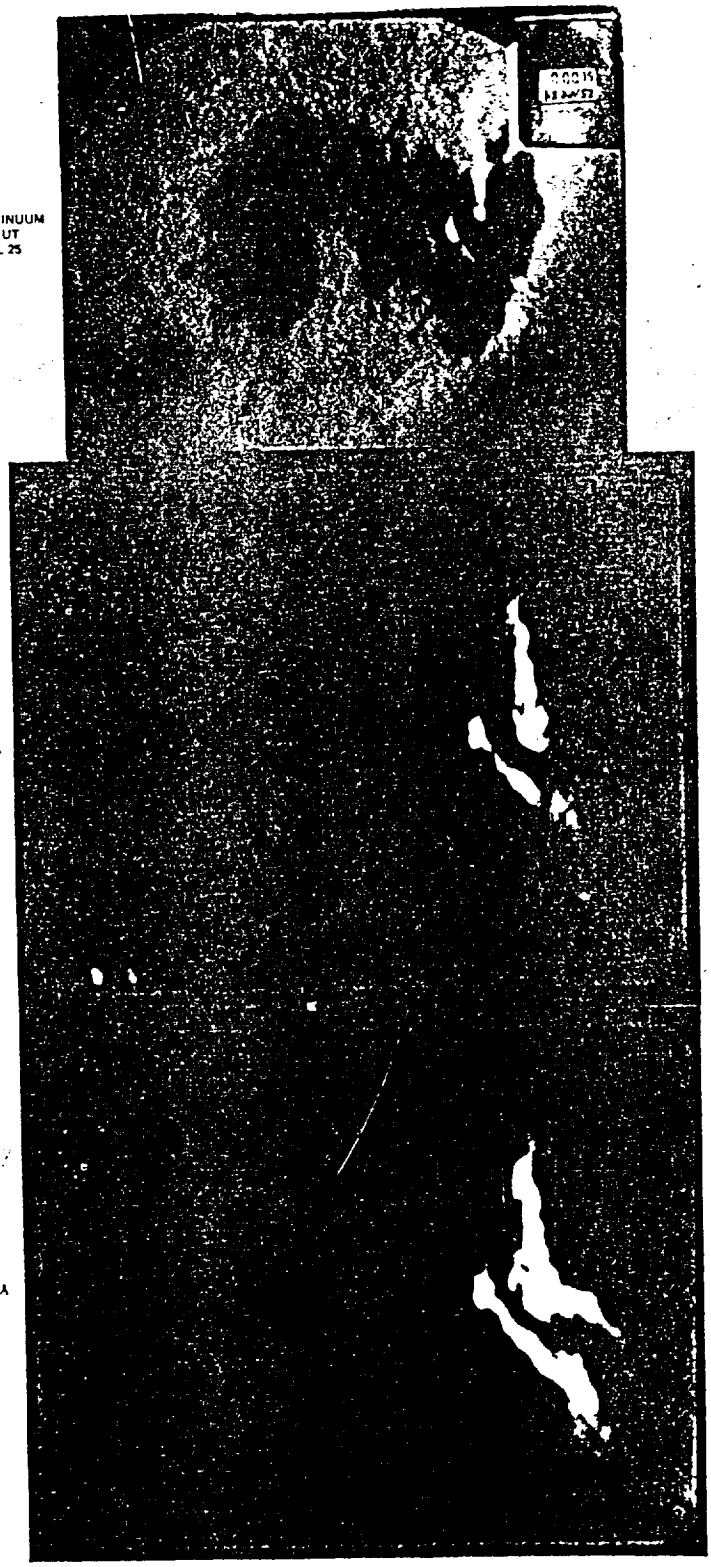

ORIGINAL PAGE IS
OF POOR QUALITY

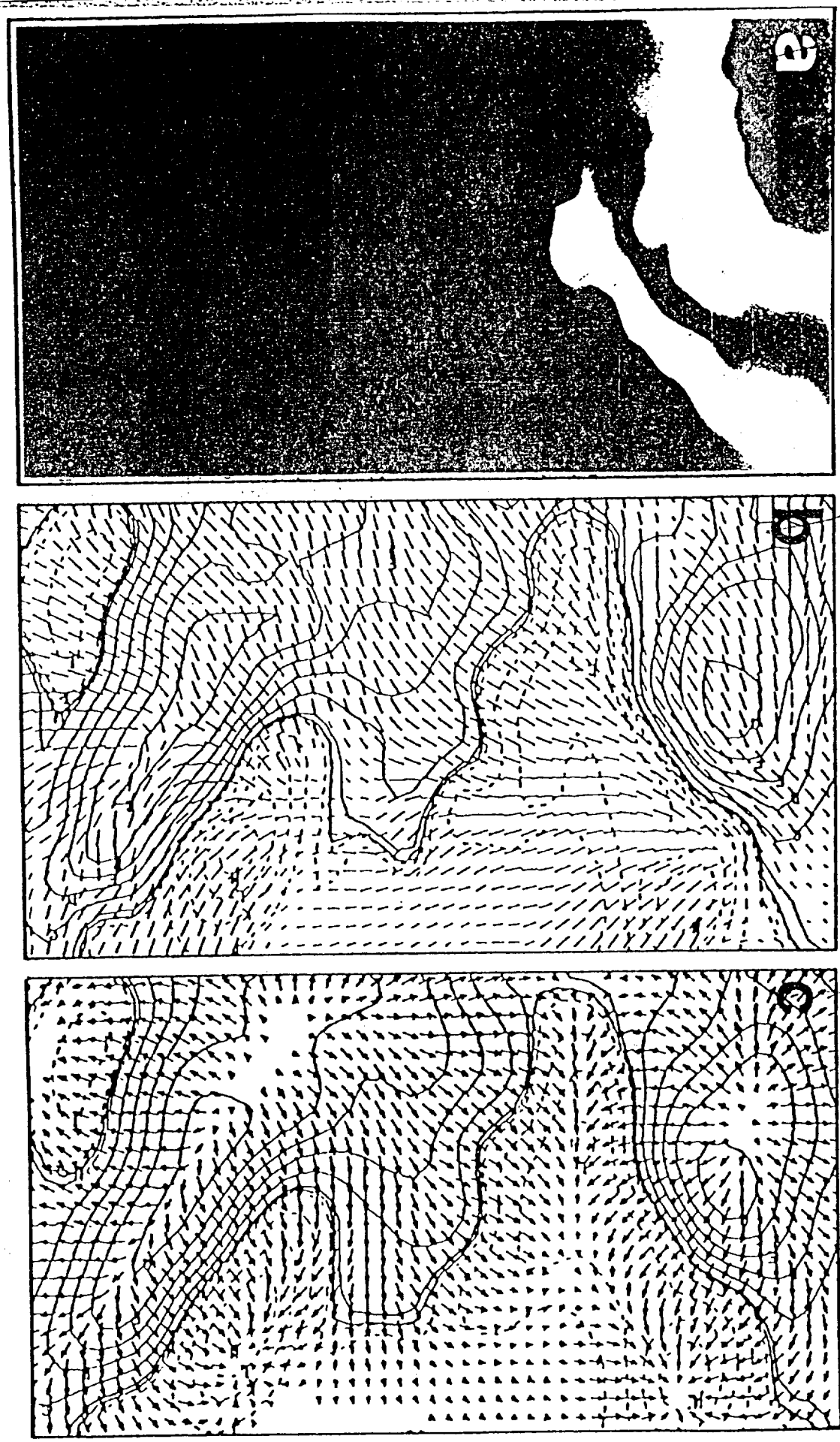

Fig. 3 ↑ top

ORIGINAL PAGE IS
OF POOR QUALITY

Fig. 4

IMAGE PLANE SHEAR MAP

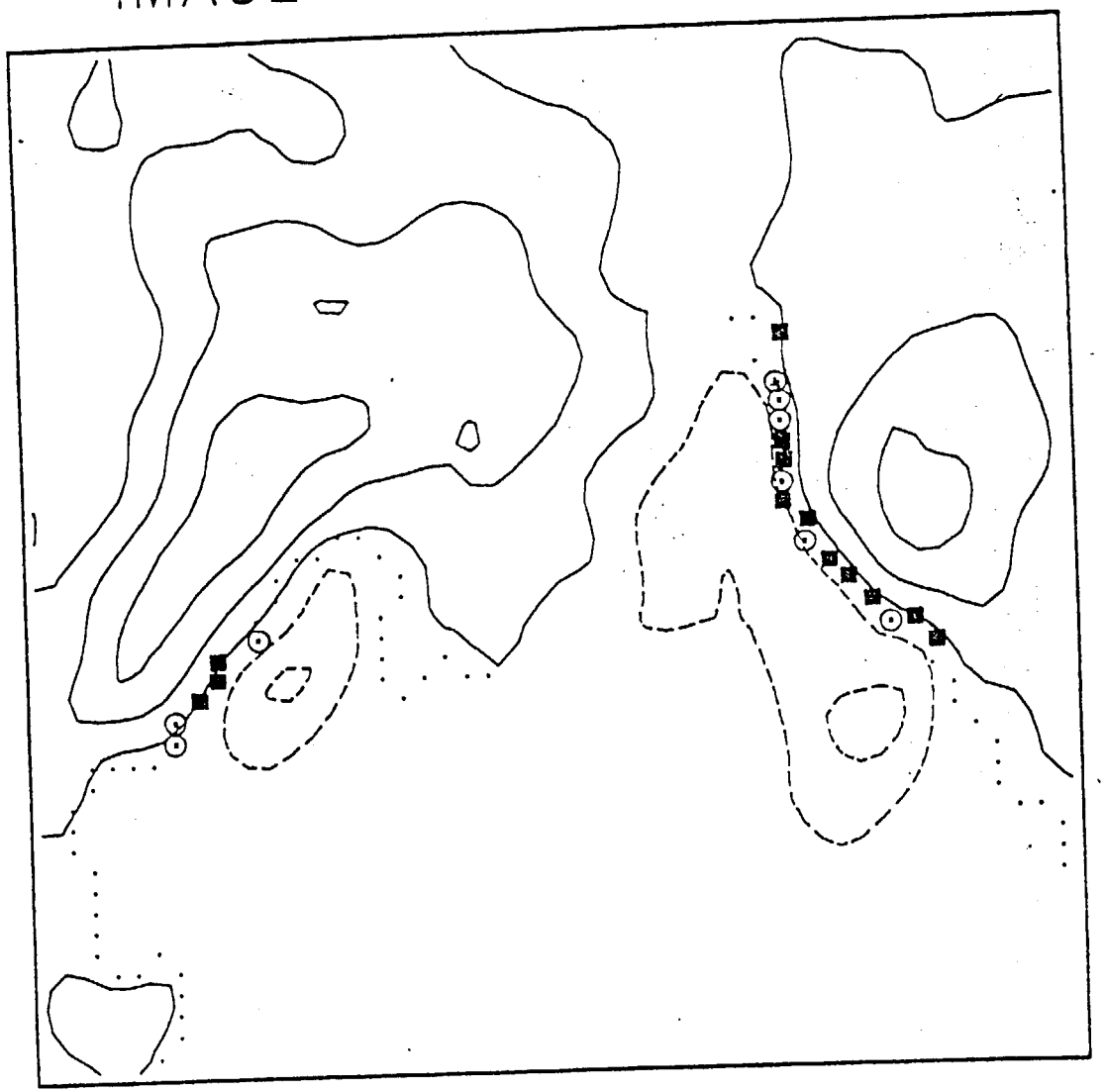

22 : 36 U T APRIL 24

ORIGINAL PAGE IS
OF POOR QUALITY

Fig. 5.

IMAGE PLANE SHEAR MAP

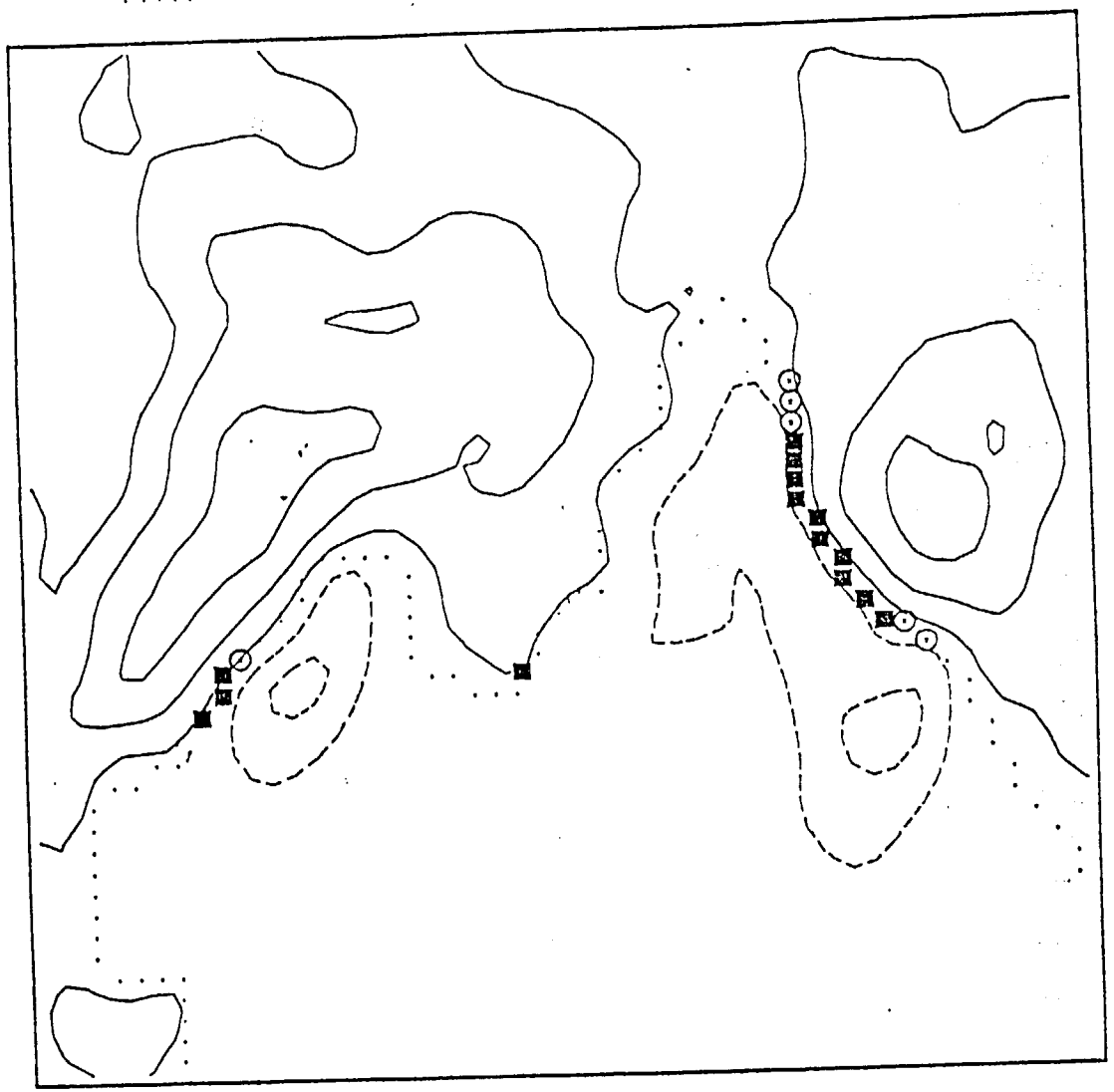

22:11 UT APRIL 24

ORIGINAL PAGE IS
OF POOR QUALITY

FIG. 6

IMAGE PLANE

~~APRIL 28~~ SHEAR MAP

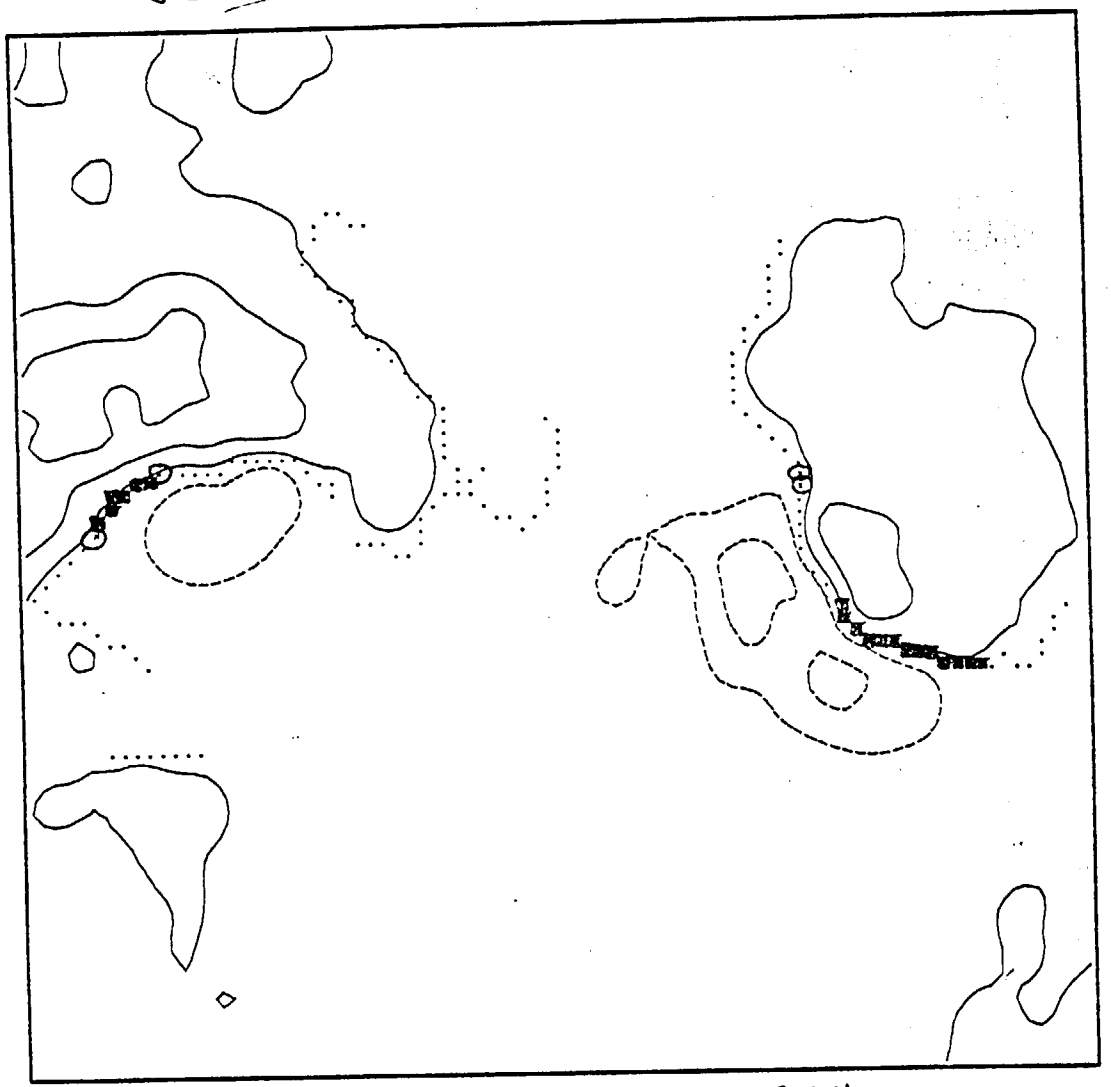

19:53 UT APRIL 28, 1984

Replace small ×× with ⊙

" large XX with ■

ORIGINAL PAGE IS
OF POOR QUALITY

~~4 of 5~~

Fig. 7

IMAGE PLANE SHEAR MAP

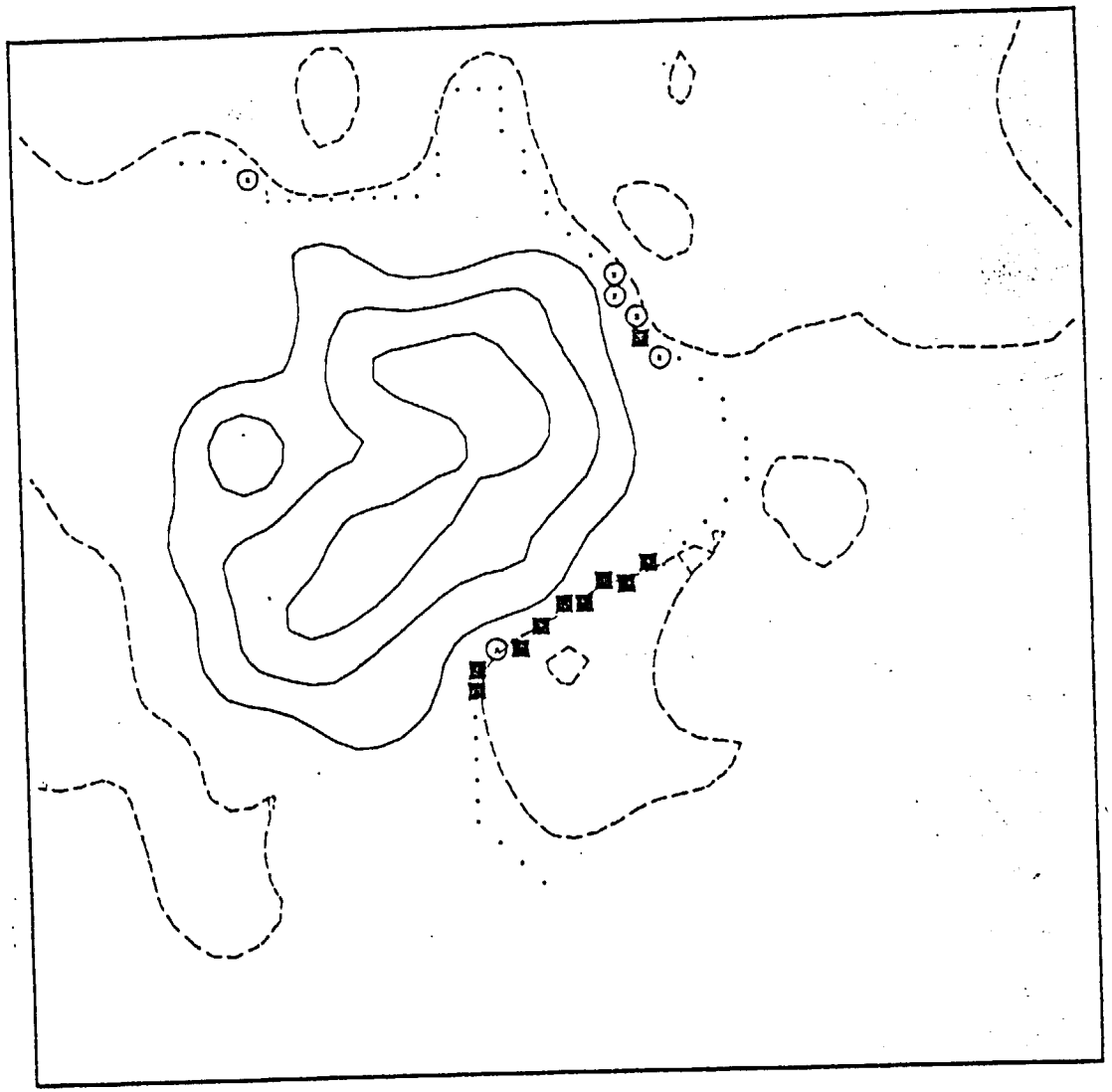

16:42 UT FEBRUARY 3, 1986

ORIGINAL PAGE IS
OF POOR QUALITY

FIG- 8

IMAGE PLANE SHEAR MAP

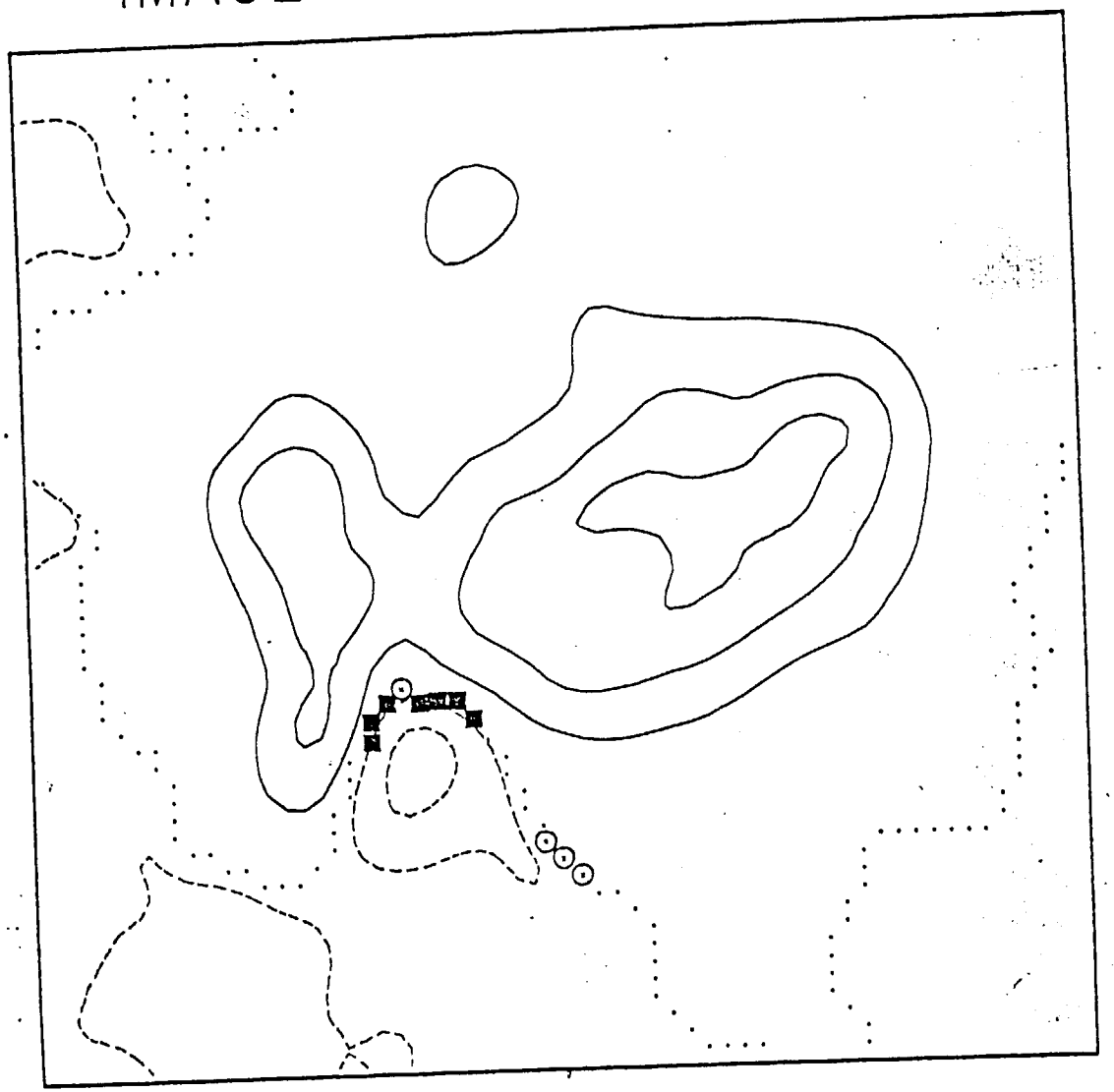

14:23 UT NOVEMBER 5, 1980

ORIGINAL PAGE IS
OF POOR QUALITY

FIG-0

FIG-9.

IMAGE PLANE SHEAR MAP

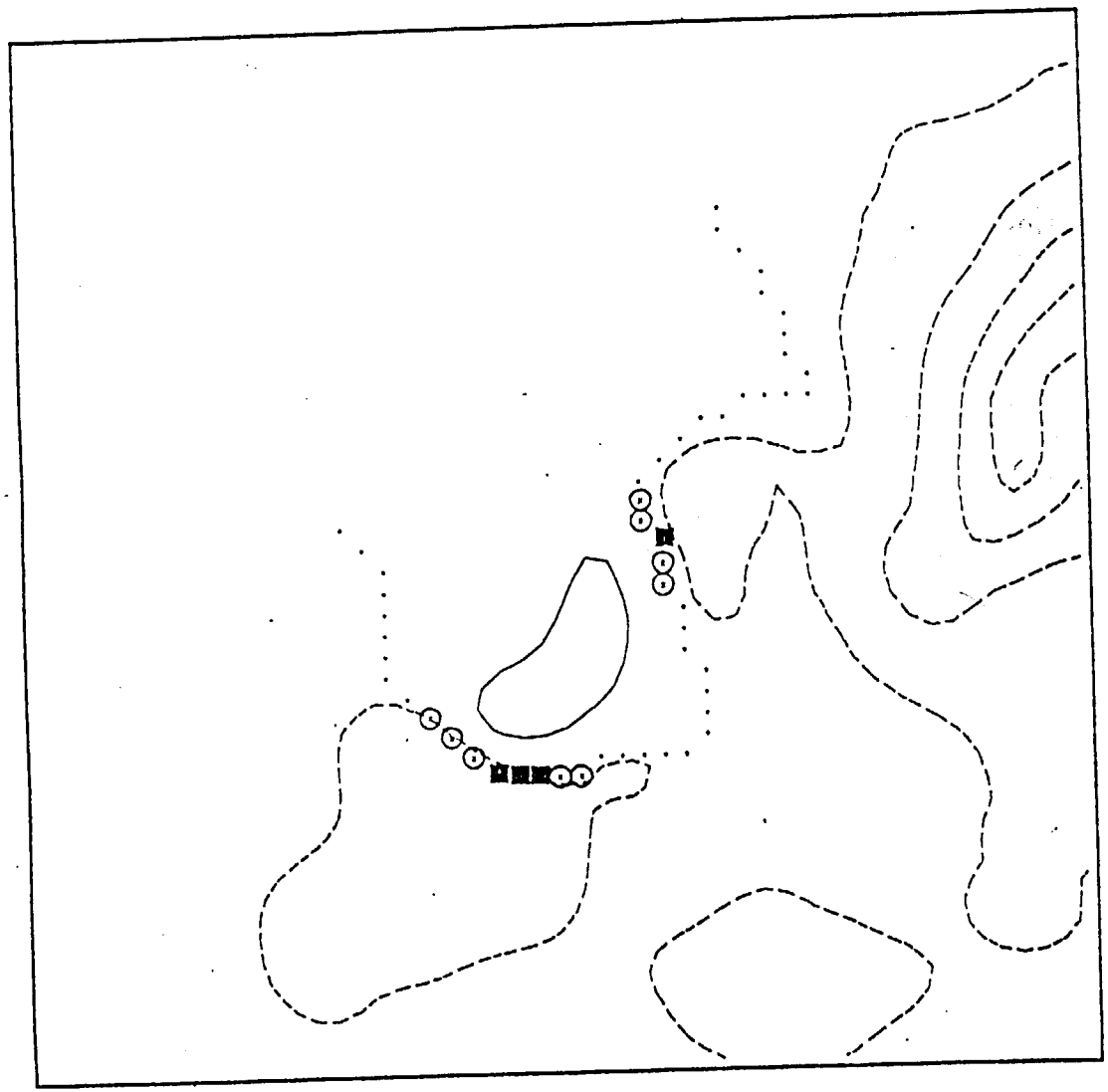

21:10 UT APRIL 6, 1980

ORIGINAL PAGE IS
OF POOR QUALITY